J. Membrane Biol. 42, 281–300 (1978)

Allosteric Cotransport of Sodium, Chloride, and Calcium by the Intestine of Freshwater Prawns

Gregory A. Ahearn

Department of Zoology, University of Hawaii, Honolulu, Hawaii 96822

Received 29 November 1977; revised 20 March 1978

Summary. The apical membrane of the intestinal epithelium of the freshwater prawn, *Macrobrachium rosenbergii*, has been found to possess an apparently unique allosteric carrier mechanism for the simultaneous cotransport of sodium, chloride, and calcium from mucosal solution to cytosol. Influxes of the two monovalent ions individually were sigmoidal functions of their respective luminal concentrations, and their kinetics followed the Hill equation for homotropic cooperativity between identical binding ligands. Increased influx of chloride sigmoidally stimulated enhanced influx of sodium, suggesting the occurrence of heterotropic cooperativity between the dissimilar ligands. Calcium entry displayed hyperbolic (Michaelis-Menten) kinetics, and this cation was found to act both as an allosteric activator of sodium entry on the shared carrier system by associating with a discrete divalent cation binding site, as well as functioning as a possible competitive inhibitor of the monovalent cation binding process. Chloride was neither an allosteric activator nor inhibitor, but appeared to function mainly as an affinity modifier of the allosteric protein for sodium.

Cotransport, or simultaneous unidirectional transmembrane transfer of dissimilar binding ligands associated with a shared carrier protein, occurs in gastrointestinal organs from a wide variety of animal species. This process has been most widely studied in cases where an ion, generally sodium, is cotransported across a cell membrane in conjunction with amino acids [1, 6, 7, 17], sugars [9, 16, 20], and vitamins [11]. Ion-ion cotransport has also been reported for mammalian ileal epithelium where sodium and chloride are simultaneously transferred across the apical cell membrane by a shared transport system [23, 25, 28]. All examples of cotransport that have been reported for gastrointestinal organs have been concerned with carrier systems which exhibit Michaelis-Menten binding kinetics. In most instances association of one ligand to the shared carrier either increases the binding affinity or the maximal transport velocity of the other ligand by stabilizing the carrier conformation or inducing structural changes that make the ternary complex more suitable for membrane translocation. In no instance has

0022-2631/78/0042-0281 $04.00

there been a description of a transport mechanism in animal gut that involves the simultaneous membrane transfer of more than two dissimilar ligand species.

This study is an extension of previous work [2, 4, 5] suggesting that sodium-chloride cotransport in the midgut of the freshwater prawn, *Macrobrachium rosenbergii*, involves an apparently unique allosteric gastrointestinal transfer mechanism where both ligands exhibit binding cooperativity. The present results indicate that calcium ion is also cotransported on this carrier system as a third binding ligand and serves as an allosteric activator of the transport protein.

Materials and Methods

The ionic composition and osmotic pressure of standard intestinal incubation medium were based on data obtained from flame photometry, chloride titration, and osmometry of hemolymph and intestinal content samples taken from freshly collected specimens of the freshwater prawn, *Macrobrachium rosenbergii*. This saline had a pH of 7.4, an osmotic pressure of 430 mosmol/kg, and consisted of the following ion concentrations in mM: Na, 221.1; K, 8.1; Ca, 12.0; Mg, 4.8; Cl, 211.3; SO_4, 25.1; PO_4, 0.4; HCO_3, 0.7. When saline of altered sodium or calcium concentration was used, potassium or choline served as the substitute cations, while sulfate was employed as a chloride replacement. Mannitol was added, where necessary, to maintain proper osmotic conditions. All experiments were conducted at a saline temperature of approximately 24 °C.

Intestines were removed from prawns, flushed gently with saline to remove fecal contents, mounted on epoxy-coated stainless steel needles, and immersed in 10 ml of aerated incubation medium in a Lucite chamber [3]. The mounted gut was subsequently perfused with saline by using a Buchler peristaltic pump at a flow rate of approximately 150 µl min^{-1}. Ion influx across the apical membrane of the intestinal epithelium was measured by briefly exposing the mucosal surface to saline containing either ^{22}Na, ^{36}Cl, or ^{45}Ca (New England Nuclear Corp. or ICN Radioisotopes) for periods of time ranging from 7.5 sec to 16 min, depending upon the luminal concentration of the labeled ion species. These exposure intervals have previously been shown to be an adequate means of establishing unidirectional ion flow across the mucosal pole of the epithelium [5]. The serosal bath contained normal concentrations of sodium (221 mM), chloride (211 mM), and calcium (12 mM) at all times except during experiments using 275 mM sodium where identical concentrations of this ion were used on both sides of the gut. Following the rinse the tissue was removed from the perfusion chamber, digested in Protosol Tissue Solubilizer (New England Nuclear Corp.), and analyzed for its radioactivity content by using a toluene-based scintillation cocktail and Beckman scintillation counter. Radioactivity in the rinsed tissue was considered to represent labeled ions in both cellular and extracellular compartments, the former increasing in isotope concentration with time, and the latter containing a fixed concentration in equilibrium with the bulk luminal solution throughout the incubation interval. The influx values in this report are expressed on the basis of intestinal serosal surface area (cm^2) determined by considering the intestine a cylinder.

Results

Time Course of Epithelial Ion Accumulation

The accumulation of sodium, chloride, and calcium by the intestinal epithelium were linear functions of time over selected exposure intervals (Fig. 1, left). In all cases a positive vertical axis intercept was obtained by

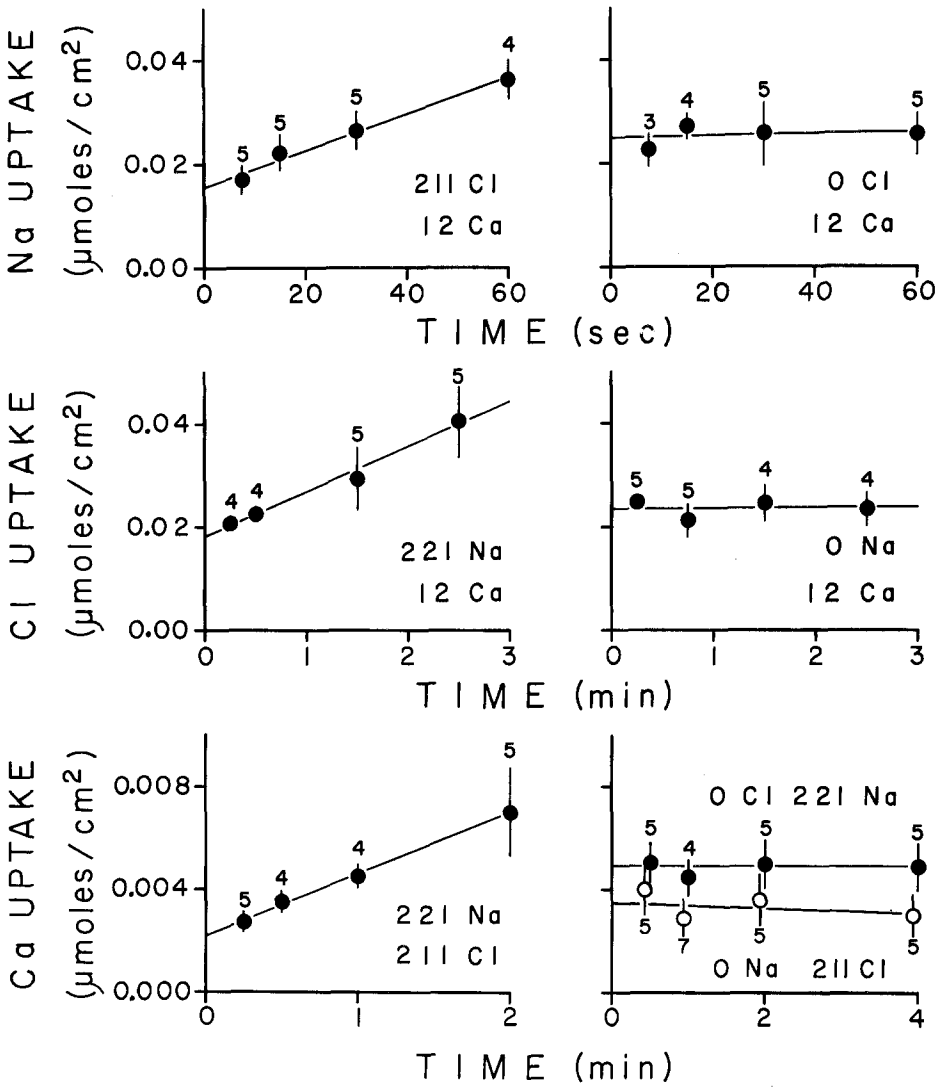

Fig. 1. Time course of ^{22}Na, ^{36}Cl, and ^{45}Ca accumulation by freshwater prawn intestine. Ion concentrations in figure refer to those in the perfusate, while control saline was present at all times in the serosal bath. Circles represent means, vertical lines are ± 1 SEM, and numbers signify sample size. Note different time scales on horizontal axes

extrapolating the uptake curve to zero time, which provided an index of extracellular radioactivity throughout a given test period for each ion. Similar means of estimating the extracellular component of tissue ion accumulation have recently been presented by Mullen and Biber [23] for sodium uptake by frog skin. Influxes of ^{22}Na, ^{36}Cl, and ^{45}Ca across the apical cell membrane of the intestinal epithelium from mucosal solution to cytosol were determined by regression analysis from the slopes of the tissue accumulation curves. Influxes of the respective ions were: J_{mc}^{Na}, 1.26 ± 0.20 (19); J_{mc}^{Cl}, 0.71 ± 0.23 (17); and J_{mc}^{Ca}, 0.14 ± 0.04 (18) μmoles cm^{-2} $hr^{-1} \pm 1$ SEM (sample size). The entry rate of each ion under these control conditions was highly significant ($P < 0.01$). Identical time course experiments for each of these ions were conducted at a variety of luminal ion concentrations. Influxes calculated from the slopes of these uptake curves are presented throughout this report. Although a high degree of statistical variability was encountered, vertical axis intercepts for the three ion species examined increased in an approximately linear fashion with an elevation in luminal ion concentration. Use of vertical axis intercepts to estimate extracellular solute concentration in the present study compares favorably with results of previous work on this same tissue using ^{3}H-inulin, $^{35}SO_4^{2-}$, and ^{3}H-mannitol as extracellular space markers [3, 13].

Figure 1 (right) indicates that when luminal chloride ion was totally replaced with sulfate (0 mM Cl; filled circles), the influxes of both sodium and calcium ceased. Similarly, when luminal potassium replaced sodium (0 mM Na), chloride and calcium (open circles) entries were abolished. In all three cases the influxes of each ion in the complete absence of the respective counterion was not significantly different than zero ($P \gg 0.05$), indicating that tissue radioactivity under these conditions was restricted only to the extracellular space. Since luminal chloride is necessary to support the unidirectional transmembrane transport of both sodium and calcium, and the transfer of chloride itself across the same membrane is totally dependent upon the presence of luminal sodium, these results suggest that all three ions share a common apical membrane carrier mechanism.

Small, but significant, increases in vertical axis intercepts occurred using saline solutions which replaced single ions (Fig. 1, right). Previous work estimating midgut extracellular space using $^{35}SO_4^{2-}$ in the marine shrimp, *Penaeus marginatus*, in normal and sodium-free salines, showed that this tissue compartment increased approximately 2% when the incubation medium lacked this cation [1]. In the present study the estimated extracellular radioactivity remaining in the tissue following the

standard rinsing procedure occupied a noncellular volume of approximately 3% of the tissue. An increase in this extracellular volume to 5% due either to cellular shrinkage or paracellular expansion in experiments involving saline lacking specific ions would be sufficient to account for the slightly elevated vertical axis intercepts. Since slopes of uptake curves are used to estimate cellular influx, alterations in the vertical intercepts due to small changes in extracellular space should not significantly influence the determination of transmembrane transport.

Sodium Transfer across the Apical Cell Membrane

Figure 2 describes sodium influx as a function of luminal sodium concentration under three test conditions. When the luminal saline contained 211 mM Cl and 12 mM Ca (control conditions), sodium influx was a sigmoidal function of luminal [Na]. Reducing mucosal [Cl] to 50 mM, while maintaining normal levels of calcium (12 mM), resulted in a shift of the sigmoidal sodium influx curve down somewhat and to the right. In contrast, with unaltered mucosal [Cl], removing calcium from the luminal perfusate (12 mM Ca on serosal side of preparation) shifted the sodium entry curve up and to the left. Although J_{mc}^{Na} at any luminal [Na] was markedly reduced when mucosal [Cl] was decreased, the

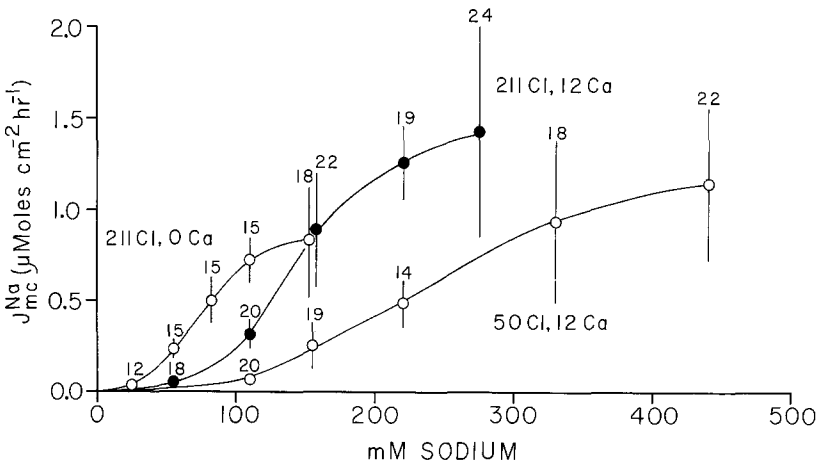

Fig. 2. Effect of luminal ion composition on sodium influx across apical cell membrane. Ion concentrations refer to those in the perfusate, while control saline was present at all times on the serosa. Symbols are as described in Fig. 1. Each mean was calculated from the slope of a separate time-course experiment, as described in Fig. 1, at the luminal ion concentrations indicated

sodium influx curve at 50 mM Cl tended to approach the normal maximal transport rate at very high concentrations of sodium. Eliminating mucosal calcium had the effect of increasing J_{mc}^{Na} over control values at all luminal [Na] up to 165 mM, but markedly reduced the maximal rate of sodium entry.

In order to determine the quantitative changes in sodium transport constants (K_t^{Na}, luminal [Na] resulting in one-half maximal influx; J_{max}^{Na}, maximal rate of sodium transfer across the apical membrane) which were induced by alterations in luminal [Cl] and [Ca], the data from Fig. 2 were converted to Augustinsson-Hofstee plots as shown in Fig. 3 in accordance with the theoretical treatment for the linear representation of multisite allosteric enzyme kinetics described by Segel [29]. The resulting kinetic constants taken from the slopes and vertical intercepts are summarized in Table 1. These figures indicate that lowering luminal [Cl] induced a significant ($P<0.001$) increase in K_t^{Na}, as well as a small, but significant ($P<0.01$), reduction in J_{max}^{Na}. Furthermore, elimination of luminal calcium ion significantly ($P<0.001$) reduced both K_t^{Na} and J_{max}^{Na}.

Using the maximal sodium influx values (J_{max}^{Na}) determined with the Augustinsson-Hofstee plots at the three test conditions (Table 1), the sigmoidal J_{mc}^{Na} data were converted to linear relationships when plotted as

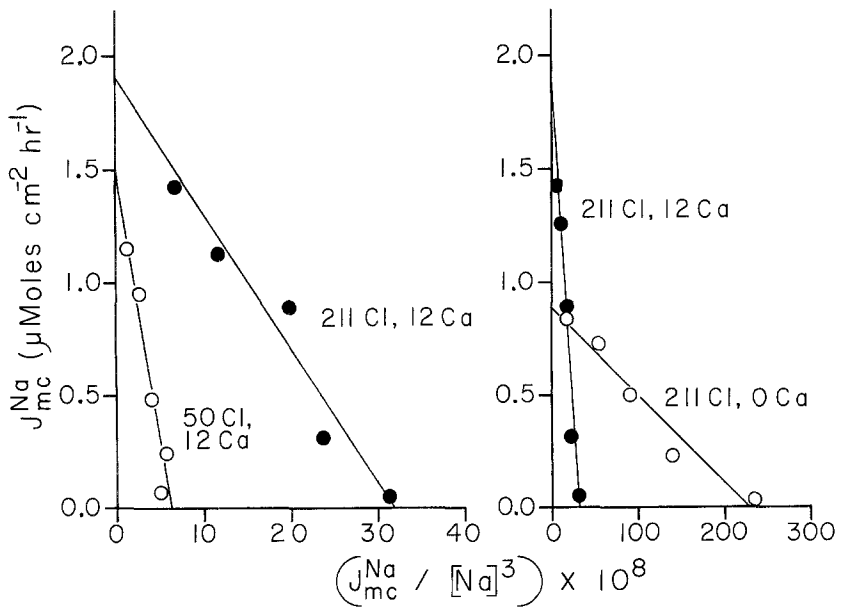

Fig. 3. Augustinsson-Hofstee plots of sodium influx as a function of luminal sodium concentration. Circles represent mean influx values derived from Fig. 2, and lines drawn through data were calculated by regression analysis

Table 1. Summary of sodium, chloride, and calcium influx constants[a]

Transported ion species	Luminal saline conditions (mM)[b]	K_t (mM)	J_{max} (μmoles cm^{-2} hr^{-1})	n
	211 Cl, 12 Ca (control)	181±8 (5)	1.90±0.16 (5)	2.98±0.11 (5)
Na	50 Cl, 12 Ca	287±35 (5) ($P<0.001$)	1.49±0.18 (5) ($P<0.01$)	3.07±0.12 (5) ($P>0.05$)
	211 Cl, 0 Ca	73±3 (5) ($P<0.001$)	0.89±0.06 (5) ($P<0.001$)	3.18±0.15 (5) ($P>0.05$)
Cl	221 Na, 12 Ca	102±5 (4)	0.76±0.08 (4)	3.22±0.12 (4)
Ca	221 Na, 211 Cl	7.7±1.1 (5)	0.23±0.02 (5)	0.63±0.04 (5)

[a] Values are means ±1 SEM, numbers in parentheses represent mean sample size, and significance figures are comparisons with control conditions.
[b] Control saline conditions (221 mM Na, 211 mM Cl, 12 mM Ca) present at all times on serosal surface.

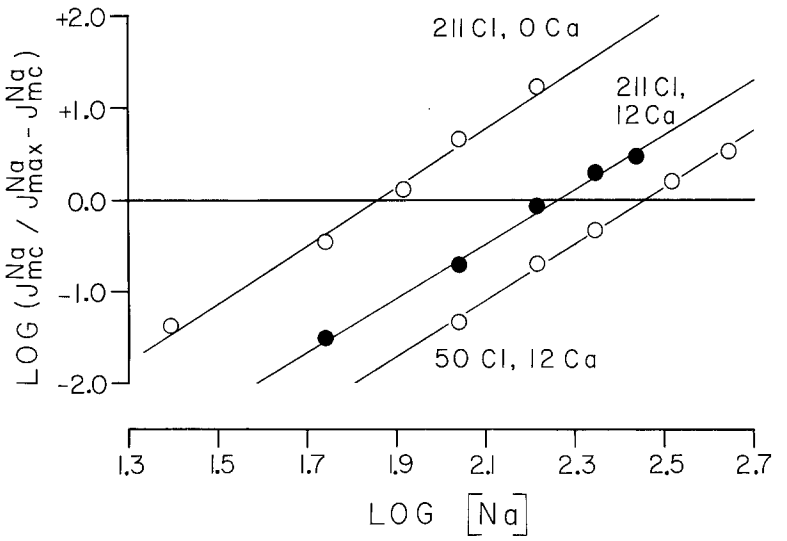

Fig. 4. Hill plots of sodium influx as a function of luminal sodium concentration. Circles represent mean influx values and were calculated from data presented in Fig. 2. Lines were calculated by regression analysis

$\log [J_{mc}^{Na}/J_{max}^{Na} - J_{mc}^{Na}]$ *vs.* $\log [Na]$ (Fig. 4). In all three cases regression lines calculated from these log-log transformations were highly significant ($P<0.01$) and suggested that the influx of sodium into the intestinal epithelium follows the Hill equation for homotropic cooperativity be-

tween identical binding ligands on a multisite binding protein:

$$\log [J_{mc}^{Na}/J_{max}^{Na} - J_{mc}^{Na}] = n_{Na} \log [Na] - \log K_t^{Na} \quad (1)$$

where J_{mc}^{Na}, J_{max}^{Na}, and K_t^{Na} have been previously defined and n_{Na} is the slope of a log-log plot and represents an index of the number of interacting sodium binding sites and their strength of interaction. At all three luminal ion conditions the interaction coefficients (n_{Na}) were not significantly different than 3.0 ($P > 0.05$) (Table 1), suggesting that, although alterations in chloride or calcium concentrations in the lumen may affect either the sodium influx binding affinity (K_t^{Na}) or maximal transport velocity (J_{max}^{Na}), such changes in these ions apparently do not influence the number of sodium binding sites or the strength of their interaction.

Chloride Transfer across the Apical Cell Membrane

At constant luminal concentration of sodium (221 mM) and calcium (12 mM), J_{mc}^{Cl} was a sigmoidal function of mucosal chloride concentration (Fig. 5, left). An Augustinsson-Hofstee plot of these data (Fig. 5, right) provided information concerning the concentration of chloride resulting

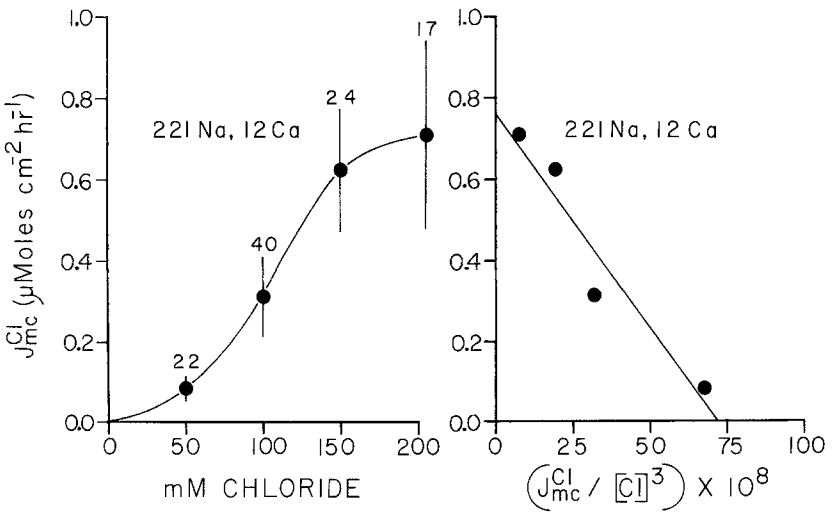

Fig. 5. *Left:* Effect of luminal chloride concentration on chloride influx across the apical cell membrane. All symbols and methods of measuring influx are as previously described. *Right:* Augustinsson-Hofstee plot of chloride influx as a function of luminal chloride concentration. Circles represent mean influx values taken from the left portion of figure and line was calculated by regression analysis

in one-half maximal influx (K_t^{Cl}) as well as a quantitative evaluation of maximal chloride entry (J_{max}^{Cl}) (Table 1). Comparison between these kinetic constants for J_{mc}^{Na} and J_{mc}^{Cl} under control luminal conditions indicates that, although the binding affinity of the epithelium for chloride is greater than that for sodium (K_t^{Na}, 181 ± 8; K_t^{Cl}, 102 ± 5 mM), the maximal entry rate of the anion is only one-half that of the cation (J_{max}^{Na}, 1.90 ± 0.16; J_{max}^{Cl}, 0.76 ± 0.08 μmoles cm^{-2} hr^{-1}). The value of J_{max}^{Cl} determined from the Augustinsson-Hofstee plot (Fig. 5, right) was used in a log-log transformation of the sigmoidal chloride entry data. A linear relationship occurred between $\log [J_{mc}^{Cl}/J_{max}^{Cl} - J_{mc}^{Cl}]$ *vs.* $\log [Cl]$ (Fig. 6), which suggests that chloride influx, like that of sodium entry, follows the homotropic cooperativity binding equation:

$$\log [J_{mc}^{Cl}/J_{max}^{Cl} - J_{mc}^{Cl}] = n_{Cl} \log [Cl] - \log K_t^{Cl} \tag{2}$$

where all the constants are defined as those for sodium influx, except that in this instance they pertain to entry of anion. The interaction coefficient for chloride transport (n_{Cl}) was not significantly different than 3.0 ($P > 0.05$) (Table 1), suggesting that both sodium and chloride influxes occur using the same number of ligand binding sites.

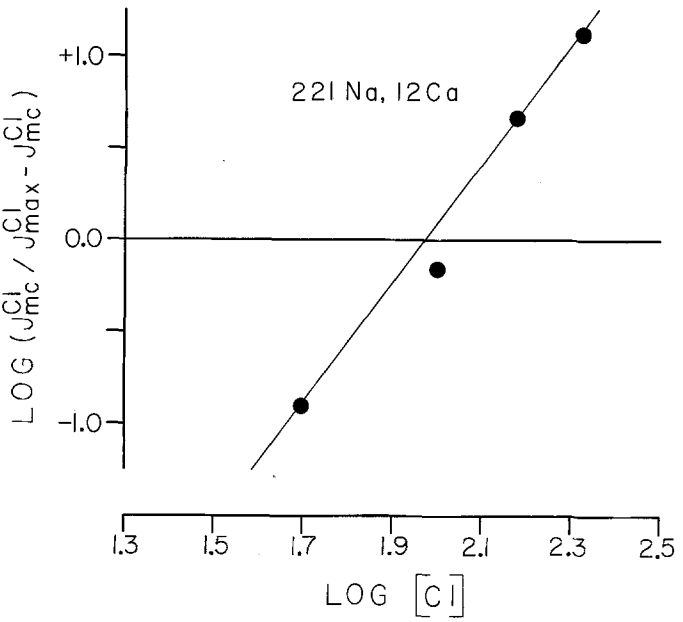

Fig. 6. Hill plot of chloride influx as a function of luminal chloride concentration. Circles represent mean influx values and were calculated from data in the left portion of Fig. 5. Line drawn through data was calculated by regression analysis

Interactions between Sodium and Chloride Influxes

Influxes of ^{22}Na and ^{36}Cl were determined in separate experiments using luminal [Na] of 55, 110, 165, and 221 mM and constant luminal [Cl] and [Ca] of 211 and 12 mM, respectively. Control ion concentrations (221 mM Na, 211 mM Cl, 12 mM Ca) were present at all times on the serosal surface. The resulting entry rates of the two ions are plotted against one another in Fig. 7. At low luminal concentrations of cation (55 mM Na), both sodium and chloride entry rates were very low (J_{mc}^{Na}, 0.052 ± 0.015; J_{mc}^{Cl}, 0.080 ± 0.024 μmoles $cm^{-2}\ hr^{-1}$) and exhibited a flux ratio (J_{mc}^{Na}/J_{mc}^{Cl}) of 0.65. Under these conditions approximately two chloride ions entered the tissue for every sodium ion. Elevation of luminal [Na] to 165 mM results in a marked acceleration in sodium entry with a considerably smaller change in anion influx (J_{mc}^{Na}, 0.888 ± 0.308; J_{mc}^{Cl}, 0.227 ± 0.052 μmoles $cm^{-2}\ hr^{-1}$), giving a flux ratio of 3.91 and implying that approximately 4 cations were entering the tissue for every anion. Further

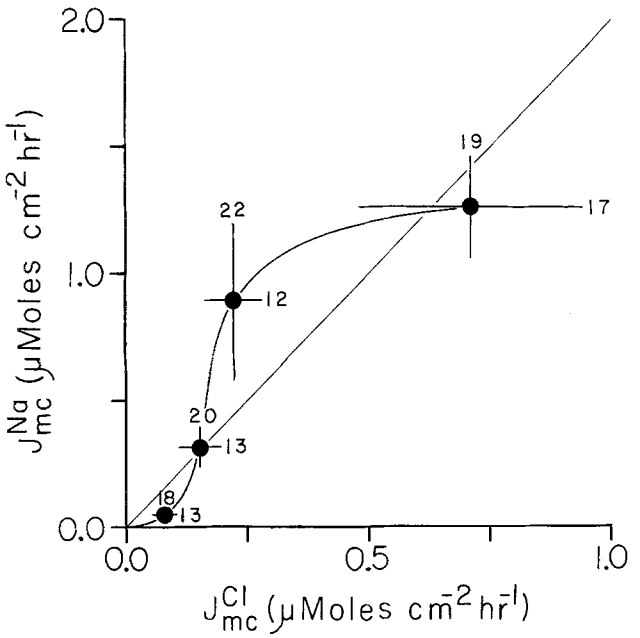

Fig. 7. Stimulatory effect of chloride influx on sodium influx. Influx rates of each ion were measured independently at luminal sodium concentrations of 55, 110, 165, and 221 mM and constant luminal chloride and calcium concentrations of 211 and 12 mM, respectively. Circles represent mean influx values of both ions at the same luminal test conditions, vertical and horizontal lines are ±1 SEM, and numbers signify sample size. Diagonal line drawn through data has a slope of 2.0 for comparison with the stoichiometry of coupled influx at each luminal test condition

increases in luminal [Na] to 221 mM did not considerably change the amount of sodium influx (J_{mc}^{Na}, 1.260 ± 0.200 μmoles $cm^{-2}\,hr^{-1}$), but did accelerate anion entry (J_{mc}^{Cl}, 0.710 ± 0.230 μmoles $cm^{-2}\,hr^{-1}$) so that a flux ratio of 1.78 was observed which suggested that at normal luminal ion concentrations (221 mM Na, 211 mM Cl, 12 mM Ca) approximately 2 sodium ions entered the tissue for each chloride ion. These results indicate that chloride influx has a clearly sigmoidal stimulatory effect on the entry sodium and that a minimum luminal concentration of sodium (110 mM Na) is needed for chloride entry to exert this influence on transmembrane cation movements. These interactions between the influxes of anion and cation suggest that heterotropic cooperativity between dissimilar ligands occurs in this tissue where the association of one monovalent ion with its binding site facilitates the attachment of the other ion to its binding site. The overall result of this interaction is enhanced transport of both ions.

Calcium Transfer across the Apical Cell Membrane

Figure 8 (left) indicates that when normal concentrations of Na (221 mM) and Cl (211 mM) were present on both surfaces of the intestine,

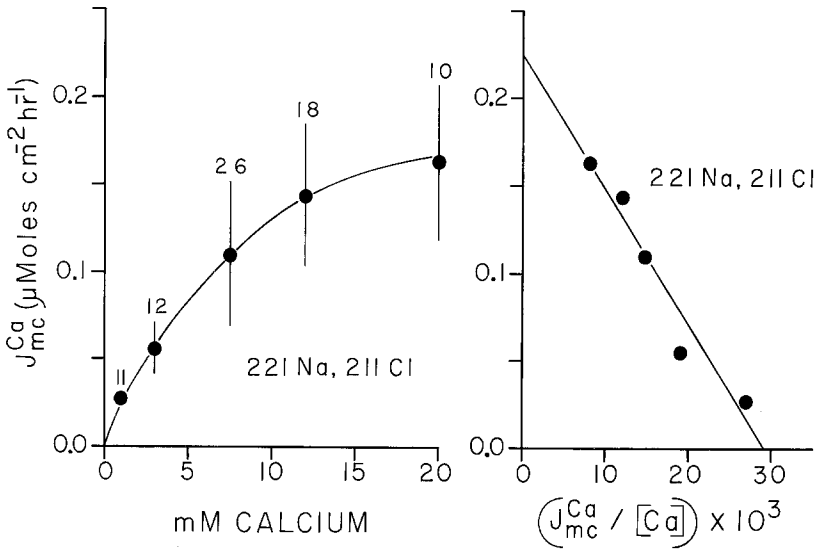

Fig. 8. *Left:* Effect of luminal calcium concentration on calcium influx across the apical cell membrane. All symbols and methods of measuring influx are as previously described. *Right:* Augustinsson-Hofstee plot of calcium influx as a function of luminal calcium concentration. Circles represent mean influx values taken from left portion of figure and line was calculated by regression analysis

J_{mc}^{Ca} was a hyperbolic function of luminal [Ca] (12 mM Ca present at all times on serosa). An Augustinsson-Hofstee plot of J_{mc}^{Ca} at variable luminal [Ca] (Fig. 8, right) was used to determine the transport constants of calcium entry under these conditions. These constants are presented in Table 1 (K_t^{Ca}, 7.73 ± 1.06 mM; J_{max}^{Ca}, 0.23 ± 0.02 μmoles cm^{-2} hr^{-1}). Using the J_{max}^{Ca} value obtained from the Augustinsson-Hofstee graph (Table 1), a log-log transformation of the hyperbolic influx data was conducted where $\log [J_{mc}^{Ca}/J_{max}^{Ca} - J_{mc}^{Ca}]$ *vs.* $\log [Ca]$ were plotted against one another. The resulting slope, the interaction coefficient n_{Ca} (0.63 ± 0.04), is presented in Table 1. The marked differences in the interaction coefficients as well as in the general kinetics of influx between calcium and the two monovalent ions suggest that considerable dissimilarities exist in the binding properties of these solutes. Both J_{mc}^{Na} and J_{mc}^{Cl} exhibit cooperativity, have n-values near 3.0, and follow the Hill equation for allosteric transfer:

$$J_{mc}^{Na} = \frac{J_{max}^{Na} [Na]^n}{(K_t^{Na})^n + [Na]^n} \quad \text{and} \quad J_{mc}^{Cl} = \frac{J_{max}^{Cl} [Cl]^n}{(K_t^{Cl})^n + [Cl]^n} \tag{3}$$

where $(K_t^{Na})^n$ and $(K_t^{Cl})^n$ represent the affinity constants modified for binding site interactions. Calcium entry, in contrast, exhibits no cooperativity, has an interaction coefficient close to 1.0, and, due to its hyperbolic character, best follows Michaelis-Menten kinetics:

$$J_{mc}^{Ca} = \frac{J_{max}^{Ca} [Ca]}{K_t^{Ca} + [Ca]}. \tag{4}$$

Discussion

The results of this report suggest that three ions, sodium, chloride, and calcium, are simultaneously cotransported across the apical membrane of the freshwater prawn intestinal epithelium on a multisite allosteric carrier protein. Within the resolving capabilities of the experimental techniques used, all three ions only appear to cross this membrane jointly (Fig. 1), implying that independent carrier processes for these ions do not exist at this epithelial pole. However, because of the inherent variability in these types of experiments, finite diffusional ion movements across this cell border probably occur but cannot, at present, be distinguished.

Application of Allosteric Protein Kinetics to Intestinal Ion Transport

Two major models have been proposed for allosteric properties of intracellular regulatory proteins. The Sequential Model by Koshland and his coworkers [21] maintains that substrate binding sites occur on different allosteric protein subunits and that each subunit can exist in either of two distinct conformations (the *R*-state and the *T*-state). Association of the substrate to the binding site converts that subunit from one conformation state to the other. The basic premise of this model is that the conversion of subunits from state to state occurs with sequential substrate binding to the individual subunits. The Concerted-Transition Model of Monod and his colleagues [22] assumes that all subunits of the allosteric protein at any given time are either in the *R*-state or the *T*-state and that conversion from one conformation to the other occurs simultaneously or in concert so that total molecular symmetry is maintained. This model proposes a pre-existing conformational equilibrium between the two states in which the different conformations have dissimilar affinities toward the ligand. The added ligand has the effect of stabilizing the conformation to which it has the highest affinity. Because of its basic premises, the Concerted-Transition Model is considerably more simple to apply to binding or transport data to verify their allosteric character and, therefore, the results of the present investigation have been analyzed using the concepts and assumptions of this model as discussed by Changeux and Rubin [14].

In an allosteric multi-subunit protein the fraction of binding sites in the total protein population occupied by a particular ligand at any ligand concentration is given by:

$$\bar{Y}=\frac{\alpha(1+\alpha)^{n-1}+L'\alpha c(1+\alpha c)^{n-1}}{(1+\alpha)^n+L'(1+\alpha c)^n} \tag{5}$$

where L' is the equilibrium ratio $(\bar{T}/\bar{R})$ between the two subunit conformational states in the absence of ligand; c is the ratio between the binding affinity of the *R*-state for the ligand and that of the *T*-state; α is the normalized substrate concentration $[S]/k_{RS}$, where $[S]$ is the observed concentration of ligand and k_{RS} the dissociation constant of the ligand from the *R*-conformation state. The fraction of protein molecules in the *R*-conformation is given by:

$$\bar{R}=1-\bar{T}=\frac{(1+\alpha)^n}{(1+\alpha)^n+L'(1+\alpha c)^n}. \tag{6}$$

When the *T*-state (low affinity conformation) has virtually no affinity for a particular ligand, the Exclusive Ligand Binding condition occurs where all solute associates with the *R*-conformation. Under these conditions Eq. (5) reduces to:

$$\bar{Y}=\frac{\alpha(1+\alpha)^{n-1}}{L'+(1+\alpha)^n} \tag{7}$$

and Eq. (6) becomes

$$\bar{R}=\frac{(1+\alpha)^n}{L'+(1+\alpha)^n}. \tag{8}$$

The coefficients L, c, k_{RS}, and α for the sodium and chloride transport data obtained in the present study were estimated by applying the procedures outlined by Changeux and Rubin [14]. Using these coefficients and the previously estimated values of n, the equations describing the best fit to the sigmoidal ion flux data were established. For both sodium and chloride transport, the Exclusive Ligand Binding condition, described by Eq. (7), best satisfies the experimental data. In Fig. 9 the influx values for sodium and chloride transfer have been converted to the notation of Monod and the sigmodial curves drawn through these points were derived from Eq. (7). In both instances the curves provide good fits to the experimental values and suggest that the Monod model for

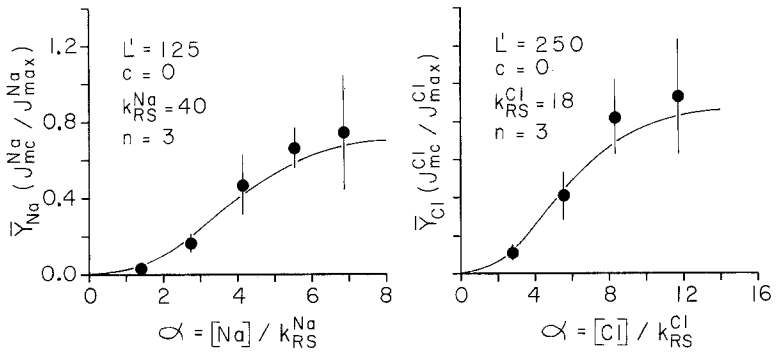

Fig. 9. Comparisons between observed sodium and chloride influxes as functions of their respective normalized luminal concentrations and expected influx values according to the Exclusive Ligand Binding condition of the Concerted-Transition Model for allosteric proteins. Influx data presented on both graphs were derived from Figs. 2 and 5 and converted to appropriate $\bar{Y}$-values. The sigmoidal lines drawn through the data on each graph were calculated using Eq. (7) and the coefficients displayed on the respective portions of the figure

allosteric protein function applies well to the sodium and chloride transfer kinetics across the apical cell membrane of the freshwater prawn intestinal epithelium.

Functional Roles of Chloride and Calcium in Allosteric Sodium Influx

An allosteric inhibitor has a higher affinity for the *T*-conformation than for the *R*-conformation and, when present together with the normal substrate, displaces the *T-R* equilibrium toward the left causing a reduction in the number of *R* binding sites for substrate attachment [22]. In contrast, an allosteric activator has its highest affinity for the *R*-state and, by binding to a site other than that utilized by the substrate, has the effect of shifting the *T-R* equilibrium to the right. Increased numbers of subunits in the *R*-state elevate substrate binding.

To determine if the effects of chloride and calcium on sodium influx (Figs. 2, 3) were due to these ions acting as either allosteric inhibitors or activators, the fraction of transport proteins in the *R*-conformation under conditions of variable luminal chloride or calcium was assessed by Eq. (8). Figure 10 indicates that the fraction of allosteric carriers in the *R*-conformation was unchanged by altering luminal chloride, but was considerably increased when the calcium concentration of the lumen was elevated from zero to 12 mM. Table 2 shows that the allosteric constant, *L*, which describes the ratio between the two conformational protein states, decreases markedly when luminal calcium is present, indicating a major shift in proteins to the *R*-state, but remains unchanged by lowering chloride in the lumen.

These results suggest that calcium represents an allosteric activator of sodium influx, whereas chloride appears to be neither an allosteric activator nor inhibitor. The functional role played by the anion in sodium influx, as shown in Table 2, appears to be mainly restricted to affecting the affinity of the cotransport carrier for the sodium ion. Increasing the chloride concentration from 50 to 211 mM decreases the dissociation constant, k_{RS} (increases the binding affinity), for sodium influx from 75 to 40 mM. This effect of the anion on sodium binding affinity probably is a result of electrostatic or conformational alterations in the sodium site induced by the anion binding at a nearby chloride site. Alterations in sodium binding are also induced by the presence of luminal calcium (Table 2). These effects appear to be independent of the

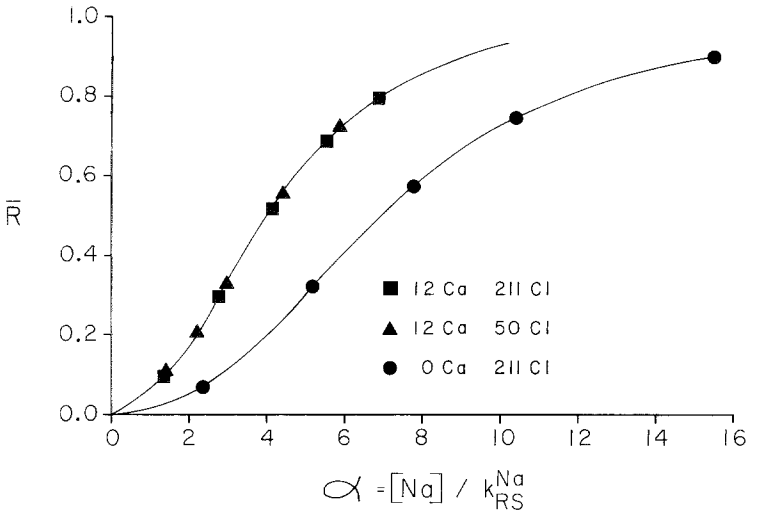

Fig. 10. Effect of luminal ion composition on the fraction of allosteric carriers in the *R*-conformation at different normalized luminal concentrations of sodium. Sodium influx data for each test conditions derived from Fig. 2 were converted to appropriate $\bar{R}$-values using Eq. (8) after determination of the allosteric coefficients L, k_{RS}, c, and α as described in Fig. 9 and in the text

Table 2. Effects of luminal ion composition on Monod transport constants of sodium influx[a]

Luminal saline conditions (mM)	L'	k_{RS} (mM Na)
211 Cl, 12 Ca (control	125	40
50 Cl, 12 Ca	125	75
211 Cl, 0 Ca	500	11

[a] Values determined according to Changeux and Rubin [14]. Control saline conditions (211 mM Na, 211 mM Cl, 12 mM Ca) present at all times on serosal surface of preparations.

allosteric activating influence of the divalent cation on sodium transport. Increasing the concentration of the divalent cation from zero to 12 mM results in a fourfold decrease in sodium binding affinity, probably due to competitive interactions between sodium and calcium at the sodium binding site.

Proposed Molecular Model for Allosteric Cotransport

The following is a tentative working model for allosteric ion cotransport across the apical pole of the prawn intestinal epithelium which

considers the transport kinetics obtained in the present study and their interpretation in terms of the Exclusive Ligand Binding Concerted-Transition Model of Monod and his colleagues. The ions, sodium, chloride, and calcium all appear to be translocated across this membrane on a shared carrier process that probably possesses three monomeric subunits (as indicated by the n-values for J_{mc}^{Na} and J_{mc}^{Cl}, Table 1), and that bears two distinctly different types of binding sites. One type of site is cooperative and apparently can be either anionic or cationic in nature to allow the independent association of both sodium and chloride. Because the maximal transport velocity for sodium influx is approximately twice that of chloride (Table 1), there are most likely on each subunit two anionic binding sites to accommodate sodium for each cationic site binding chloride. The other type of binding site is noncooperative and allows for the association of the allosteric activator, calcium. Because sodium and chloride influxes display heterotropic cooperativity (Fig. 7), their individual binding sites may be spatially quite close to one another on a single protein subunit so that potential inhibitory electrostatic forces are minimized for the binding of one ion by the previous attachment of the other. The binding site for calcium must be in a location that can lead to a major conformational change in protein structure following its attachment in order to convert the oligomer from the low affinity T-state to the high affinity R-state (Fig. 10, Table 2) and thereby increase the transmembrane transfer of the monovalent ions.

Comparisons with Other Gastrointestinal Ion Transport Systems

The intestine of the freshwater prawn is apparently the first reported gastrointestinal organ from any animal shown to display an allosteric cotransport carrier mechanism for the simultaneous transmembrane transfer of three different ion species. The guts of several vertebrates exhibit coupling between the epithelial transport of sodium and that of chloride. The bullfrog intestine [8, 26], bovine rumen [15], and rat colon [10] all possess a combination of coupled sodium-chloride transfer mechanisms as well as independent systems for transmural transport of these two monovalent ions. These studies, however, did not provide a detailed analysis of the transport events occurring at either the apical or basal poles of the respective epithelial cells and therefore were unable to identify, with certainty, the site or kinetics of the processes responsible for the observed transport coupling.

Rabbit ileum possesses both a coupled sodium-chloride influx process as well as a mechanism for the independent transapical transfer of sodium ion alone [18, 25, 27]. Detailed analysis of the coupled transport process for sodium and chloride on the apical membrane disclosed hyperbolic influx kinetics for both ions [24]. A one-for-one stoichiometry occurred between the entry rates of these solutes on this shared carrier, and a model was advanced which indicated a random combination of sodium and chloride with the membrane protein to form a ternary complex with the restriction that only the unloaded carrier and ternary complex were capable of translocation across the mucosal membrane. A similar coupled influx process for the electrically silent transmembrane transfer of NaCl across the mucosal border of the rabbit gallbladder has also been recently demonstrated [19]. None of these authors found a regulatory role for exogenous calcium in monovalent ion binding to these cotransport carrier proteins as was disclosed in the present study concerning the allosteric cotransport of sodium and chloride in prawn gut (Figs. 2, 10, Table 2). However, intracellular calcium appears to have a regulatory function in transapical monovalent ion transport in rabbit ileum. Bolton and Field [12] found that the application of calcium ionophore A23187 to the serosal surface of this tissue resulted in a loss of net sodium-chloride absorption coincident with an increase in the secretion of these two ions. It was suggested that elevated intracellular calcium concentration due to ionophore-stimulated influx was responsible for the alteration in monovalent ion transfer, but the mechanism by which calcium exerts this effect was not disclosed.

These comparisons between species suggest that there may be at least two ways in which calcium may regulate monovalent ion transport in gastrointestinal organs as well as possibly in other types of epithelial cells. The divalent cation may act as a binding cofactor at the carrier protein step, increasing both the binding affinity of the carrier for monovalent ions (through appropriate conformational changes) and its subsequent transmembrane transfer. In contrast, calcium may also act intracellularly in an unknown manner to reverse the direction of net monovalent ion transport, presumably through interactions at the apical pole of the epithelial cell.

This investigation was supported by the National Science Foundation under grant numbers BMS 74-20663 and PCM 76-84105.

References

1. Ahearn, G.A. 1976. Co-transport of glycine and sodium across the mucosal border of the midgut epithelium in the marine shrimp, *Penaeus marginatus*. *J. Physiol. (London)* **258**:499
2. Ahearn, G.A. 1977. Allosteric cooperativity during intestinal sodium and chloride transport in freshwater prawns. *Proc. Int. Union Physiol. Sci.* **13**:13
3. Ahearn, G.A., Maginniss, L.A. 1977. Kinetics of glucose transport by the perfused midgut of the freshwater prawn, *Macrobrachium rosenbergii*. *J. Physiol. (London)* **271**:319
4. Ahearn, G.A., Maginniss, L.A., Song, Y.K., Tornquist, A. 1977. Intestinal water and ion transport in freshwater malacostracan prawns (*Crustacea*). *In*: Water Relations in Membrane Transport in Plants and Animals. A.M. Jungreis, T. Hodges, A.M. Kleinzeller, and S.G. Schultz, editors. p. 129. Academic Press, New York
5. Ahearn, G.A., Tornquist, A. 1977. Allosteric cooperativity during intestinal cotransport of sodium and chloride in freshwater prawns. *Biochim. Biophys. Acta* **471**:273
6. Alvarado, F., Mahmood, A. 1974. Cotransport of organic solutes and sodium ions in the small intestine: A general model. Amino acid transport. *Biochemistry* **13**:2882
7. Alvarez, O., Goldner, A.M., Curran, P.F. 1969. Alanine transport in rabbit jejunum. *Am. J. Physiol.* **217**:946
8. Armstrong, W.McD., Quay, J.F. 1971. Sodium and chloride transport by isolated amphibian intestine. *In:* Intestinal Transport of Electrolytes, Amino Acids, and Sugars. W.McD. Armstrong and A.S. Nunn, editors. p. 79, Charles C. Thomas, Springfield
9. Bihler, I. 1969. Intestinal sugar transport: Ionic activation and chemical specificity. *Biochim. Biophys. Acta* **183**:169
10. Binder, H.J., Rawlins, C.L. 1973. Electrolyte transport across isolated large intestinal mucosa. *Am. J. Physiol.* **225**:1232
11. Berger, E., Long, E., Semenza, G. 1972. The sodium activation of biotin absorption in hamster small intestine *in vitro*. *Biochim. Biophys. Acta* **255**:873
12. Bolton, J.E., Field, M. 1977. Ca ionophore-stimulated ion secretion in rabbit ileal mucosa: Relation to actions of cyclic 3′, 5′-AMP and carbamylcholine. *J. Membrane Biol.* **35**:159
13. Brick, R.W., Ahearn, G.A. 1978. Lysine transport across the mucosal border of the perfused midgut in the freshwater shrimp, *Macrobrachium rosenbergii*. *J. Comp. Physiol.* **124**:169
14. Changeux, J. Rubin, M.M. 1968. Allosteric interactions in aspartate transcarbamylase. III. Interpretation of experimental data in terms of the model of Monod, Wyman, and Changeux. *Biochemistry* **7**:159
15. Chien, W., Stevens, C.E. 1972. Coupled active transport of Na and Cl across forestomach epithelium. *Am. J. Physiol.* **223**:997
16. Crane, R.K. 1968. Absorption of sugars. *In*: Handbook of Physiology, C.F. Code, editor, Vol. III, Chap. 69; p. 1323, American Physiology Society, Washington, D.C.
17. Curran, P.F., Schultz, S.G., Chez, R.A., Fuisz, R.E. 1967. Kinetic relations of the Na-amino acid interaction at the mucosal border of intestine. *J. Gen. Physiol.* **50**:1261
18. Frizzell, R.A. 1976. Coupled sodium-chloride transport by small intestine and gallbladder. *In:* Intestinal Ion Transport. J.W.L. Robinson, editor. p. 101, University Park Press, Baltimore
19. Frizzell, R.A., Dugas, M.C., Schultz, S.G. 1975. Sodium chloride transport by rabbit gallbladder. Direct evidence for a coupled NaCl influx process. *J. Gen. Physiol.* **65**:769

20. Goldner, A.M., Schultz, S.G., Curran, P.F. 1969. Sodium and sugar fluxes across the mucosal border of rabbit ileum. *J. Gen. Physiol.* **53**:362
21. Koshland, D.E., Nemethy, G., Filmer, D. 1966. Comparison of experimental binding data and theoretical models in proteins containing subunits. *Biochemistry* **5**:365
22. Monod, J., Wyman, J., Changeux, J. 1965. On the nature of allosteric transitions: A plausible model. *J. Mol. Biol.* **12**:88
23. Mullen, T.L., Biber, T.U.L. 1978. Sodium uptake across the outer surface of the frog skin. *In:* Membrane Transport Processes. J.F. Hoffman, editor. Vol. 1, p. 99. Raven Press, New York
24. Nellans, H.N., Frizzell, R.A., Schultz, S.G. 1973. Coupled sodium-chloride influx across the brush border of rabbit ileum. *Am. J. Physiol.* **225**:467
25. Nellans, H.N., Frizzell, R.A., Schultz, S.G. 1974. Brush-border processes and transepithelial Na and Cl transport by rabbit ileum. *Am. J. Physiol.* **226**:1131
26. Quay, J.F., Armstrong, W.McD. 1969. Sodium and chloride transport by isolated bullfrog small intestine. *Am. J. Physiol.* **217**:694
27. Schultz, S.G., Frizzell, R.A. 1977. Effect of cyclic-adenosine-monophosphate on chloride transport across some mammalian epithelia. *In:* Biochemistry of Membrane Transport. G Semenza and E. Carafoli, editors. p. 225. Academic Press, New York
28. Schultz, S.G., Frizzell, R.A., Nellans, H.N. 1974. Ion transport by mammalian small intestine. *Annu. Rev. Physiol.* **36**:51
29. Segel, I.H. 1975. Enzyme Kinetics. John Wiley & Sons, New York